Differential mitochondrial proteomic analysis of A549 cells infected with avian influenza virus subtypes H5 and H9

Yuting Yang
Hunan Normal University
Yun Zhang
Hunan Normal University
Changcheng Yang
Hunan Normal University
Fang Fang
Hunan Normal University
Ying Wang
Hunan Normal University
Haiyan Chang (changhaiyanw@163.com)
Hunan Normal University
Ze Chen
Hunan Normal University
Ping Chen
Hunan Normal University

Research

Keywords: Influenza virus, Mitochondria, Two-dimensional electrophoresis, Proteomics

Posted Date: September 1st, 2020

DOI: https://doi.org/10.21203/rs.3.rs-60533/v1

Version of Record: A version of this preprint was published on February 18th, 2021. See the published version at https://doi.org/10.1186/s12985-021-01512-4.

Abstract

Background

In the past 20–30 years, both the highly pathogenic avian influenza (HPAI) H5N1 and low pathogenic avian influenza (LPAI) H9N2 viruses have been reported to cross species barriers to infect humans. However, H5N1 viruses could cause severe damage and a high death rate, but H9N2 viruses could not. In this study, we use H9N2 virus infection as a control to investigate the differential expression of mitochondrial-related proteins caused by H5N1 and H9N2 virus infections in A549 cells.

Methods

According to the determined viral infection titer, A549 cells were infected with 1 MOI (multiplicity of infection) virus, and the mitochondria were extracted after 24 hours of incubation. The lysed mitochondrial protein was analyzed by BCA method for protein concentration, SDS-PAGE preliminary analysis, two-dimensional gel electrophoresis, and mass spectrometry. Select different protein spots, perform Western Blot to verify the proteomics results, and then perform GO and KEGG analysis.

Results

In the 2-D gel electrophoresis analysis, 227 protein spots were detected in the H5N1-infected group, and 169 protein spots were detected in the H9N2-infected group. After further MS identification and removal of redundancy, 32 differentially expressed proteins were identified. Compared with the H9N2 group, the H5N1-infected group had 16 upregulated mitochondrial proteins and 16 downregulated proteins. The 70 kDa heat shock protein analogs, short-chain enoyl-CoA hydratase, malate dehydrogenase, and ATP synthase were verified by Western Blot, and the results were consistent with proteomics.

Conclusions

Functional analysis indicated that these differentially expressed proteins were involved mainly in apoptosis, metabolism and the cytoskeleton. The differential expression of eight mitochondrial proteins in H5N1-infected cells resulted in decreased T cell activation, decreased antigen presentation and stress response, reduced ATP synthesis, and decreased induction of apoptosis, resulting in the higher pathogenicity of H5N1 virus than H9N2 virus.These finding may provide a basis for analyzing the pathogenesis of influenza viruses with different virulence levels, identifying anti-influenza host targets and developing new influenza vaccines.

Background

H5N1, an influenza A virus (IAV), is a highly pathogenic avian influenza (HPAI)virus. It was first isolated and identified in domestic geese in Guangdong Province, China, in 1996. The spread of H5N1 avian influenza illness in poultry populations increases the risk of human infection [1]. In May 1997, the first human H5N1 virus infection occurred in the Hong Kong Special Administrative Region of China: 18 people were infected, and 6 died. As of 2019, the H5N1 IAV has migrated to at least 17 countries, and has caused 861 confirmed infections and 455 deaths in humans [2]. Human infections with HPAI H5N1 viruses mainly lead to serious pneumonia, with a high mortality of approximately 53%. H9N2, another IAV, is a low pathogenic avian influenza (LPAI) virus [3]. Individuals infected with LPAI H9N2 viruses generally have a mild upper respiratory tract illness, with only one death to date.

Influenza virus induces caspase-dependent apoptosis, by activating caspase-3 [4]. Apoptosis is divided into the extrinsic pathway and intrinsic pathways. The intrinsic apoptotic pathway engages caspases via members of the BCL-2 protein family and mitochondria in response to severe cellular damage or stress [5]. Mitochondria also play a leading role in the release of many important apoptosis-inducing molecules due to mitochondrial outer membrane permeabilization (MOMP) [6]. According to a whole-cell proteomic study of A549 cells infected with avian influenza virus H7N9 and influenza virus H1N1, some differentially expressed proteins are localized to mitochondria [7]. Differences in viral virulence may be related to apoptosis. Influenza virus is a high-risk virus that poses a great threat to human health and the economy. According to its virulence level, IAVs are further divided into HPAI and LPAI, viruses: HPAI viruses are generally H5 and H7 subtypes, and LPAI viruses are mainly H9 and H10 subtypes. HPAI viruses, pose the greatest threat to human life.

Therefore, we selected LPAI H9N2 virus-infected A549 cells as the control group and HPAI H5N1 virus-infected A549 cells as the test group in this study. Two-dimensional difference gel electrophoresis (2D) and MALDI-TOF tandem mass spectrometry (MS/MS) were applied to investigate the differences in the host proteome after infection with these two influenza virus strains and to explore the different pathogenic mechanisms of H5N1 and H9N2 in infected human cells.

Materials And Methods

Virus Tissue Culture Infective Dose (TCID)

A/Chicken/Jiangsu/07/2002 (H9N2), and A/Chicken/Henan/12/2004 (H5N1) were obtained from the Wuhan Institute of Virology, Chinese Academy of Sciences. The A549 cells were uniformly inoculated into a 48-well plate with a cross-hatching design. The virus was diluted 10-fold with a virus dilution solution[8], and 100 μL of virus solution was added to each well for 1 h and incubated in a cell culture incubator at 37 ℃, with 5% CO_2 and saturated humidity. The virus was then aspirated. After culture for 24 h, the median TCID ($TCID_{50}$) was calculated by the method of Reed and Muench [9]. From the of $TCID_{50}$ value, we calculated the multiplicity of infection (MOI) by the following formula.

$$MOI = \frac{0.7\mathrm{TCID}_{50}}{Cell}$$

Cell Culture and Infection

A549 non-small cell lung cancer cells were purchased from the Cell Resource Center of the Shanghai Academy of Sciences, Chinese Academy of Sciences.

Human lung epithelial A549 cells were cultured in F-12K Nutrient Mixture (GIBCO, Grand Island, NY, USA) at pH 7.2, supplemented with 10% fetal bovine serum (GIBCO) and penicillin (100 U/mL)/streptomycin (100 μg/mL) and grown in a cell culture incubator at 37 ℃, under conditions of 5% CO_2 and saturated humidity. A549 cells (80% confluent) were infected with H5N1 and H9N2 viruses at an MOI of 1 for 1 h, and culture medium was added at 24 h.

Extraction of Mitochondrial Proteins from Virus Infection

Virus-infected cells were washed once with precooled PBS, and lysis buffer (25 mM mannitol, 0.5 mM EGTA, 5 mM HEPES, 0.1% BSA [w/v]) was added. The cells were scraped and placed in a homogenizer for homogenization. The cells were then transferred to a 50 mL screw-cap tube and centrifuged for 5 min at 4 ℃ and 600 × g, and the supernatant was removed. The cells were transferred to a new 50 mL round-bottom tube, centrifuged to pellet cell debris and nuclear proteins, and centrifuged again. The supernatant obtained by centrifugation in the previous step was centrifuged at 10,300 g for 10 min at 4 ℃, and the precipitate was mitochondrial protein. Centrifugation was repeated once, and the precipitate was combined with that obtained in the previous step to further maximally enrich mitochondrial protein. The obtained mitochondrial protein was suspended in acetone precooled to -20 ℃, stored at -20 ℃ for 12 h or more, and centrifuged at 8750 g for 35 min at 4 ℃. The supernatant was then removed, and the centrifugation step was repeated once. On an ultraclean work bench, samples were naturally air-dried on ice, and an appropriate amount of lysate was added to fully dissolve the precipitate. Protein was further dissolved by vortexing.

The sample was collected and the protein concentration was determined using a BCA protein assay kit (Sangon Biotech, Shanghai, China) according to the manufacturer's instructions. The samples were then aliquoted and stored at − 80 ℃ until subsequent use.

Two-Dimensional (2-D) Gel Electrophoresis

Rehydration solution (8 M urea; 2 M thiourea; 4.0% [w/v] CHAPS; 20 mM Tris base; 20 mM DL-dithiothreitol; 0.5% [v/v], pH 3–10 amidine, and 10% [v/v] bromophenol blue) was added to the protein sample. For isolation of proteins by isoelectric focusing(IEF), a salt bridge was formed at the two poles of the electrophoresis tank, the supernatant of the centrifuged protein sample was added uniformly to the electrophoresis tank, and the isoelectric focusing strip was removed from the − 20 ℃ freezer (17 cm, pH 3–10) and equilibrated to room temperature. The sample was added to the electrophoresis channel, and the appropriate amount of mineral oil was added to cover the strip. The program was set as follows: 50 V for 14 h, passive rehydration; 500 V for 1 h, linear; 1000 V for 1 h, rapid; 5000 V for 1 h, rapid; 8000 V for

1 h, linear; and rapid ramping to 8000 V for 60,000 Vh [10]. After isoelectric focusing, strips were equilibrated in equilibration buffer (6 M urea, 20% glycerol, 2% SDS, 25 mM Tris-HCl [pH 8.8]) containing 0.2% (w/v) dithiothreitol for 15 min and then in the same buffer containing 3.0% (w/v) iodoacetamide and 0.175% (v/v) bromophenol blue for 15 min. Separation in the second direction was performed via 12.5% SDS-PAGE under a constant current of 25 mA, and gels were stained with Coomassie Brilliant Blue G-250. After decolorization, analysis was performed using ImageMaster software to match gel spots, and gray values that were significantly different (gray value ≥ 2.0-fold) between the H9N2-infected and H5N1-infected groups were selected for MS analysis.

In-gel Trypsin Digestion, MS and Data Searching

The sample was mixed in an equal ratio with 10 mg/mL α-cyano-4-hydroxcinnamic acid, directly spotted onto a spotting plate, and allowed to dry at room temperature. Peptide mass spectra were obtained with a 5800 MALDI TOF/TOF mass spectrometer (AB SCIEX, Foster City, USA). The MS/MS data of the peptide mass fingerprint (PMF) were submitted to the online software Mascot (Matrix Science, Boston, MA, USA) for identification according to the NCBIProt database [10].

Western Blot Analysis

The extracted total cell lysate and mitochondrial proteins of H5N1 and H9N2 virus-infected A549 cells were quantified with a BCA kit (Sangon Biotech, Shanghai, China). Mitochondrial proteins (40 μg) and total cell lysate (40 μg) were separated by 12% SDS-PAGE and transferred to nitrocellulose membranes (BBI Life Sciences). After blocking with 5% (w/v) skim milk in TBST (50 mM Tris[pH 8.0], 150 mM NaCl, 0.1% [v/v] Tween-20) for 1 h at 37 ℃, membranes were incubated separately overnight at 4 °C with rabbit monoclonal or polyclonal antibodies against ECHS1 (ab170108), MDH2 (ab181873) (Abcam), ATP5F1 (15999-1-ap), HSPA1L (13970-1-ap), BAX (50599-2-Ig), and Caspase 3 (66470-2-Ig) (Proteintech). After three washes with TBST, membranes were incubated with horseradish peroxidase (HRP)-conjugated goat anti-rabbit IgG or HRP-conjugated goat anti-mouse IgG (used at a 1:5000 dilution, Proteintech) for 1 h at room temperature and were then washed three times with TBST. The immunoreactive protein bands were detected using enhanced chemiluminescence reagent (ECL; Advansta, CA, USA), with TOM40 (18409-1-ap) (Proteintech) and β-actin (66009-1-Ig) (Proteintech) as the loading controls.

Bioinformatics Analysis

The identified proteins were subjected to subcellular localization, functional classification, and interaction protein queries using Gene Ontology (GO) analysis, KEGG, and STRING, and related proteins or signal pathways were analyzed. The literature was used to determine the verification target [10].

Statistical Analysis

The statistical significance of differences between groups was determined by using a paired, nonparametric Student's T-test. $P < 0.05$ was considered statistically significant. The experiment was repeated three times.

Results

2D Screening and Identification of Differentially Expressed Proteins

Mitochondrial protein extracts (1500 μg) from A549 cells infected with H5N1 and H9N2 influenza viruses were loaded onto 2-D gels. Two-dimensional gel electrophoresis showed 227 protein spots in the H5N1 group (Fig. 1A) and 169 protein spots in the H9N2 group (Fig. 1B). Eight differentially expressed protein spots on the mitochondria were also illustrated in enlarged formats (Fig. 1C). After further MS identification and removal of redundancy, 32 differentially expressed proteins were identified. Compared with the H9N2-infected group, the H5N1-infected group had 16 upregulated mitochondrial proteins and 16 downregulated proteins (Table 1, Table 2). The upregulated 70-kDa heat shock protein 1-like (HSPA1L) is located in the mitochondrial matrix, and short-chain enoyl-CoA hydratase (ECHS1) is located in the inner membrane of the mitochondria. Among these downregulated proteins, stress-70 protein, malate dehydrogenase (MDH2), mitochondrial membrane ATP synthase (ATP5F1), and stomatin-like 2 protein are located in the mitochondrial inner membrane, while peroxiredoxin 5 and 60-kDa heat shock protein (HSP60) are located in the mitochondrial matrix.

Gene Ontology Analysis of Differentially Expressed Proteins

The proteins corresponding to the 32 differential protein spots were subjected to Gene Ontology analysis. Only 26 of the 32 differentially expressed proteins were annotated through data analysis. The main biological processes involving these differentially expressed proteins are shown in Fig. 2A; **65**.38% (17 proteins) were cellular components or involved in biogenesis, 61.53% (16 proteins) were involved in the positive regulation of biological processes, 50% (13 proteins) were associated with cell death, and 42.3% (11 proteins) were involved in programmed cell death. These findings indicate that the differences in the apoptotic process may be the cause of the differences in the host cells infected by different subtypes of influenza viruses. The cellular components are shown in Fig. 2B; **65**.38% (17 proteins) belonged to the organelle component. The molecular functions of the differentially expressed proteins are shown in Fig. 2C; **84**.61% (22 proteins) were involved in binding, including protein binding, DNA binding and other molecular binding functions. These findings indicate that the binding protein has an important role in infecting hosts with different subtypes of influenza viruses.

KEGG Pathway Analysis of Differentially Expressed Proteins and Construction of the Protein Interaction Network Diagram

KEGG analysis of signaling pathways involving the differentially expressed proteins was conducted. The differentially expressed proteins were involved in 37 signaling pathways, 9 of which were significantly different ($P < 0.05$) (Fig. 3). A total of 7.69% were involved in metabolic processes, of which 3.85% participated in carbohydrate metabolism, 3.85% participated in lipid metabolism, and 23.08% participated

in genetic information processes. Of that 23.08%, 7.69% participated in the transcription process; 11.54% participated in protein folding, classification, and degradation processes; 7.69% were involved in antigen processing and presentation in the immune system; 7.69% were involved in virus infection; and 7.69% participated in parasitic infection. These findings indicate that the differential proteins involved in the antigen processing and presentation of the immune system and viral infectious diseases have important roles in the differences between different subtypes of influenza virus-infected host cells.

Protein-protein interaction analysis was performed on the differentially expressed proteins using STRING online software. Of these, 24 of the 32 differentially expressed proteins were identified, and the results are shown in Fig. 4. The overall set of differentially expressed proteins is divided into three sections, and the albumin (ALB) protein connects these three sections. ALB protein is involved in mitochondrial ROS production [11]. As a node of the regulatory network, it may be play an important role in the virus infection process. At the same time, proteins essentially interact with each other. The proteins ATP5FB, MDH2, ECHS1, and HSPA1L are located in the key site of the network and play crucial roles in the difference in virulence between H5N1 and H9N2.

Western Blot of Differentially Expressed Proteins

To validate the results of the proteomic studies, we performed western blot analysis of the differentially expressed mitochondrial proteins ATP5F1, ECHS1, MDH2, and HSPA1L with the TOM40 protein as the control. The results are shown in Fig. 5; the density of the band corresponding to the mitochondrial protein MDH2 was significantly reduced in the H5N1-infected group compared with the H9N2-infected group ($P < 0.05$). In addition, the densities of the ECHS1 and HSPA1L protein bands were significantly enhanced ($P < 0.05$, for both). The ATP5F1 band was weak, but the difference was nonsignificant. We performed the same WB experiment with total cell protein, and the results are shown in Fig. 6. There were significant differences in ECHS1 and MDH2 in the total protein.

ECHS1 is associated with apoptosis; we speculate that the difference between different subtypes of influenza virus-infected hosts may be related to apoptosis. Western blotting was used to assess the total protein levels of BAX and Caspase 3 in A549 cells, with β-actin as the internal reference. The results are shown in Fig. 7. The expression of BAX was increased in both the H5N1-infected group and the H9N2-infected group and was slightly higher in the H9N2-infected group than in the H5N1-infected group. Caspase 3 (32 kDa) expression was reduced in both the H5N1-infected and H9N2-infected groups, but the difference between the two groups was nonsignificant. The total protein western blotting experiments showed that the differentially expressed proteins were mainly related to endogenous apoptosis.

Discussion

To date, many researchers have applied proteomics to study whole-cell proteomics during infection with influenza viruses such as H5N1, H3N2, and H1N1. However, we believe that compared with whole-cell proteomics, subcellular proteomics is more capable of identifying early diagnostic markers of influenza virus infection and is more conducive to the analysis of disease-related proteins and observation of the

dynamic process of host cell infection with the virus. Influenza A virus can induce apoptosis [12], and the apoptotic pathway occurs in mitochondria [13]. To study the effect of infection with two different subtypes of influenza virus on the mitochondrial proteome, thus, there is no need to set a blank control. We performed subcellular mitochondrial proteomic analysis of A549 cells infected with H5 and H9 subtype avian influenza viruses was conducted. Compared with Control, H5N1 and H9N2 basically appeared different proteins after 24 hours of infection [14–15]. In order to better study the process of virus infecting the host, we chose the 24 hours time point to study the mitochondrial protein difference between two viruses with different pathogenicity.

2-D electrophoresis allows differential distribution of many protein isotypes. After data redundancy removal, we found that 16 proteins were upregulated and 16 were downregulated in the H5N1-infected group compared with the H9N2-infected group. However, further validation of the subcellular localization of some proteins is needed. Among the identified mitochondrial proteins, 6 mitochondrial proteins were downregulated and 2 mitochondrial proteins were upregulated in the H5N1-infected group compared with the H9N2-infected group.

After GO analysis, most differentially expressed proteins were binding proteins. A variety of binding proteins have been discovered that affect the virulence of influenza viruses, such as poly (rC)-binding protein 2 and nuclear export protein 1 [16–17]. We found that these differentially expressed binding proteins may be related to the mechanism of influenza virus infection. Therefore, our findings are helpful for further analysis of the mechanism that binds proteins to influenza viruses.

Among the upregulated mitochondrial proteins was the molecular chaperone HSPA1L, a member of the 70-kDa heat shock protein (HSP70) family that is localized to the mitochondrial matrix and whose coding gene is located on chromosome 6p21 in the HLA class III region [18]. Other studies, showed that HSP70 appears to be upregulated in HPAI compared to LPAI IAVs. This chaperone is involved in a variety of cellular processes, including folding and transport of newly synthesized polypeptides, proteolytic activation of misfolded proteins, and formation and dissociation of protein complexes [19]. The ECHS1 protein is found in mitochondria, peroxisomes, and smooth endoplasmic reticulum. The upregulated protein enoyl-CoA hydratase, encoded by ECHS1 on chromosome 10, is a 160-kDa hexamer enzyme consisting of 290 amino acids and is located in the mitochondrial matrix. ECHS1 is associated with mitochondrial short-chain and medium-chain fatty acid β-oxidation and branched-chain amino acid catabolic pathways, as well as other catabolic pathways[20]. In the absence of hepatitis B virus infection, the ECHS1 gene was subjected to RNA interference, and the proapoptotic genes Bid and Bax were found to be upregulated after transfection into HepG2 cells. However, in Xiao et al.'s study in hepatitis B virus-infected HepG2 cells, ECHS1, a binding protein of hepatitis B virus surface antigen, promoted HepG2 cell apoptosis. The coexistence of ECHS1 and hepatitis B virus surface antigen changed the expression of Bcl-2 family proteins, 12 proapoptotic proteins were upregulated, and 8 antiapoptotic proteins were downregulated [21]. The results of this study are consistent with those obtained after RNA interference in the absence of hepatitis B virus infection, indicating that not all viruses can use ECHS1 as a binding protein for viral surface antigens, thereby promoting apoptosis. Related studies, have confirmed that

influenza virus can induce apoptosis. In our study, the difference in BAX expression detected by western blotting showed that the level of endogenous apoptosis induced by the highly pathogenic H5N1 virus was higher than that induced by the low pathogenic H9N2 virus. Endogenous apoptosis leads to mitochondrial swelling, disappearance of internal cristae and permeabilization, a possible reason for the difference in the virulence of these two viruses. In addition, downregulation of ECHS1 protein expression affects its fatty acid β oxidation pathway and reduces the replication ability of RNA viruses such as measles virus, vesicular stomatitis virus, and Semliki Forest virus [22]. In our results, the expression of ECHS1 protein was upregulated in the H5N1 virus-infected group compared with the H9N2 virus-infected group, which may explain why the H5N1 virus is more pathogenic than the H9N2 virus.

Among these downregulated mitochondrial proteins, the heat shock 70-kDa protein 1-like, malate dehydrogenase, mitochondrial membrane ATP synthase, and stomatin-like 2 proteins are located in the mitochondrial inner membrane, while the peroxiredoxin 5 and 60-kDa heat shock proteins are located in the mitochondrial matrix. HSPA1L indirectly affects body metabolism and biological function by regulating iron-sulfur protein maturation [23]; malate dehydrogenase is associated with the TCA cycle [24]; ATP synthase is involved in energy production and permeability transition pores (PTP, key players in cell death) ; stomatin-like protein 2 is involved in cell T cell activation, calcium homeostasis, and the stress response [25]; peroxiredoxin-5, which plays an anti-oxidative stress role in cell protection [26–27]; and 60-kDa heat shock protein is involved in controlling protein folding, the stress response, and the delivery of endogenous peptides to antigen presenting cells [28].

These eight differentially expressed mitochondrial proteins, especially ECHS1, may be used as new antiviral targets, but the results need to be further verified by a series of methods, such as RNA interference.

In IAV proteomic studies by other groups, 60-kDa heat shock protein, 70-kDa heat shock protein and ATP synthase subunits often appear as differentially expressed proteins. Is differential expression of these proteins shared by different IAVs? To date, a relatively small amount of proteomic data has been obtained for different IAVs; thus, the proteomic profiles of additional IAVs must be compared to augment this research to provide a basis for this possibility.

We hypothesized that H5N1 is highly pathogenic compared with H9N2, probably because of the upregulation and downregulation of the above eight mitochondrial proteins, which in turn inhibit T cell activation, antigen presentation, stress responses, and other processes. The increased mortality from H5N1 may also be due to metabolic abnormalities. A total of 42.3% of these differentially expressed proteins were involved in the apoptotic process, and we speculate that the altered levels of mitochondrial protein expression during IAV pathogenesis are due mainly to the difference in the endogenous apoptotic process. Our analysis also identified many other influencing factors, indicating that infection of the host cell is a complex process. Mechanistic analysis of these specific processes needs to be continuously augmented through numerous experimental studies.

Conclusions

In this study, we infected A549 cells with H5N1 of HIAV and H9N2 of LIAV, and extracted the mitochondrial proteins of the infected cells for differential protein analysis. Studies have found that the proteomics differences between H5N1 and H9N2 weaken T cell activation, antigen presentation, and stress-induced apoptosis, which may also cause a certain degree of metabolic abnormality. After GO analysis, most of these differential proteins are related to apoptosis. To a certain extent, it shows that the pathogenicity of different IAVs is related to their ability to cause apoptosis. In our research, we have identified different proteins such as Stress-70 protein, peroxide reductase-5, enoyl-CoA hydratase, Stomatin-like protein 2, ATP synthase, 60 kDa heat shock protein, etc. It plays an important role in apoptosis. It provides some help for the analysis of the pathogenic mechanism of influenza viruses with different virulence, and provides a certain reference for the selection of anti-influenza virus host targets.

Supplementary Information

Additional file 1:Table S1. Mass spectrometry data search selection criteria

Additional file 2:Table S2. TCID50 results of A549 cells infected with H5N1 influenza virus

Additional file 3:Table S3. $TCID_{50}$ results of A549 cells infected with H9N2 influenza virus

Additional file 3:Table S4. Calculation of mitochondrial protein concentrations after H5N1 infection

Additional file 3:Table S5. Calculation of mitochondrial protein concentrations after H9N2 infection

Abbreviations

AIV: Avian influenza virus; HPAI:highly pathogenic avian influenza; LPAI: low pathogenic avian influenza; 2D:Two-dimensional difference gel electrophoresis; MALDI-TOF: Matrix-Assisted Laser Desorption/ Ionization Time of Flight; GO: Gene Ontology; KEGG: Kyoto Encyclopedia of Genes and Genomes; FBS: Fetal bovine serum; NCBI: National Center for Biotechnology Information; MOI: Multiplicityof infection; PBS: Phosphate buffer saline; SD: Standard deviation.

Declarations

Acknowledgements

We thank Dr. Jian-Jun Chen from Wuhan Institute of Virology for kindly providing the A/Chicken/Jiangsu/07/2002(H9N2), A/Chicken/Henan/12/2004(H5N1) and for use of the BSL-3 facilities.

Authors' contributions

YY, YW, ZC and CH designed experiments; YY, ZY, YC carried out experiments; FF and CP analyzed experimental results; and YY wrote the manuscript.

Funding

This work was supported by the Hunan Provincial Education Department (18C0074); National Natural Science Foundation of China (Grants 31670838).

Availability of data and material

The mass spectrometry proteomics data have been deposited to the ProteomeXchange Consortium (http://proteomecentral.proteomexchange.org) via the iProX partner repository, dataset identifier PXD017921.

Ethics approval and consent to participate

Not applicable

Consent for publication

Not applicable.

Competing interests

All the authors have no conflict of interest.

References

1. Duan L, Bahl J, Smith GJD, Wang J, Vijaykrishna D, Zhang LJ, Zhang JX, Li KS, Fan XH, Cheung CL. The development and genetic diversity of H5N1 influenza virus in China, 1996–2006. Virology. 2008;380:243–54.
2. Kombiah S, Kumar M, Murugkar H, Nagarajan S, Tosh C, Senthil Kumar D, Rajukumar K, Gautam S, Singh R, Karikalan M, et al. Experimental pathology of two highly pathogenic H5N1 viruses isolated from crows in BALB/c mice. Microb Pathog. 2020;141:103984.
3. Sun Y, Liu J. H9N2 influenza virus in China: a cause of concern. Protein cell. 2015;6:18–25.
4. Qu X, Ding X, Duan M, Yang J, Lin R, Zhou Z, Wang S. Influenza virus infection induces translocation of apoptosis-inducing factor (AIF) in A549 cells: role of AIF in apoptosis and viral propagation. Arch Virol. 2017;162:1–7.
5. Ashkenazi A. Targeting the extrinsic apoptotic pathway in cancer: lessons learned and future directions. Journal of Clinical Investigation. 2015;125:487–9.
6. Tait S, Green D. Mitochondria and cell death: outer membrane permeabilization and beyond. Nat Rev Mol Cell Biol. 2010;11:621–32.

7. Ding X, Lu J, Yu R, Wang X, Wang T, Dong F, Peng B, Wu W, Liu H, Geng Y, et al. Preliminary Proteomic Analysis of A549 Cells Infected with Avian Influenza Virus H7N9 and Influenza A Virus H1N1. PloS one. 2016;11:e0156017.
8. Peng B, Peng N, Zhang Y, Zhang F, Li X, Chang H, Fang F, Wang F, Lu F, Chen Z. Comparison of the Protective Efficacy of Neutralizing Epitopes of 2009 Pandemic H1N1 Influenza Hemagglutinin. Frontiers in immunology. 2017;8:1070.
9. Biacchesi S, Skiadopoulos MH, Yang L, Murphy BR, Collins PL, Buchholz UJ. Rapid human metapneumovirus microneutralization assay based on green fluorescent protein expression. J Virol Methods. 2005;128:192–7.
10. Wang M, Chen Y, Guo Z, Yang C, Qi J, Fu Y, Chen Z, Chen P, Wang Y. Changes in the mitochondrial proteome in human hepatocytes in response to alpha-amanitin hepatotoxicity. Toxicon. 2018;156:34–40.
11. Tretter L, Mayer-Takacs D, Adam-Vizi V. The effect of bovine serum albumin on the membrane potential and reactive oxygen species generation in succinate-supported isolated brain mitochondria. Neurochem Int. 2007;50:139–47.
12. Liu B, Meng D, Wei T, Zhang S, Hu Y, Wang M. Apoptosis and pro-inflammatory cytokine response of mast cells induced by influenza A viruses. PloS one. 2014;9:e100109.
13. Hata A, Engelman J, Faber A. The BCL2 Family: Key Mediators of the Apoptotic Response to Targeted Anticancer Therapeutics. Cancer discovery. 2015;5:475–87.
14. Liu N, Song W, Wang P, Lee K, Chan W, Chen H, Cai Z. Proteomics analysis of differential expression of cellular proteins in response to avian H9N2 virus infection in human cells. Proteomics. 2008;8:1851–8.
15. Liu C, Zhang A, Guo J, Yang J, Zhou H, Chen H, Jin M. Identification of human host proteins contributing to H5N1 influenza virus propagation by membrane proteomics. J Proteome Res. 2012;11:5396–405.
16. Chutiwitoonchai N, Aida Y. NXT1, a Novel Influenza A NP Binding Protein, Promotes the Nuclear Export of NP via a CRM1-Dependent Pathway. Viruses. 2016;8.
17. Li X, Fu Z, Liang H, Wang Y, Qi X, Ding M, Sun X, Zhou Z, Huang Y, Gu H, et al. H5N1 influenza virus-specific miRNA-like small RNA increases cytokine production and mouse mortality via targeting poly(rC)-binding protein 2. Cell research. 2018;28:157–71.
18. Takahashi S, Andreoletti G, Chen R, Munehira Y, Batra A, Afzal N, Beattie R, Bernstein J, Ennis S, Snyder M. De novo and rare mutations in the HSPA1L heat shock gene associated with inflammatory bowel disease. Genome medicine. 2017;9:8.
19. Srivastava S, Vishwanathan V, Birje A, Sinha D, D'Silva P. Evolving paradigms on the interplay of mitochondrial Hsp70 chaperone system in cell survival and senescence. Crit Rev Biochem Mol Biol. 2019;54:517–36.
20. Bedoyan J, Yang S, Ferdinandusse S, Jack R, Miron A, Grahame G, DeBrosse S, Hoppel C, Kerr D, Wanders R. Lethal neonatal case and review of primary short-chain enoyl-CoA hydratase (SCEH)

deficiency associated with secondary lymphocyte pyruvate dehydrogenase complex (PDC) deficiency. Mol Genet Metab. 2017;120:342–9.

21. Xiao C, Yang X, Huang Q, Zhang Y, Lin B, Liu J, Liu Y, Jazag A, Guleng B, Ren J. ECHS1 acts as a novel HBsAg-binding protein enhancing apoptosis through the mitochondrial pathway in HepG2 cells. Cancer letters. 2013;330:67–73.
22. Takahashi M, Watari E, Shinya E, Shimizu T, Takahashi H. Suppression of virus replication via down-modulation of mitochondrial short chain enoyl-CoA hydratase in human glioblastoma cells. Antiviral research. 2007;75:152–8.
23. Stehling O, Paul V, Bergmann J, Basu S, Lill R. Biochemical Analyses of Human Iron-Sulfur Protein Biogenesis and of Related Diseases. Methods Enzymol. 2018;599:227–63.
24. Kombiah S, Kumar M, Murugkar H, Nagarajan S, Tosh C, Senthil Kumar D, Rajukumar K, Gautam S, Singh R, Karikalan M, et al. Experimental pathology of two highly pathogenic H5N1 viruses isolated from crows in BALB/c mice. Microb Pathog. 2020;141:103984.
25. Giorgio V, Burchell V, Schiavone M, Bassot C, Minervini G, Petronilli V, Argenton F, Forte M, Tosatto S, Lippe G, et al. Ca binding to F-ATP synthase β subunit triggers the mitochondrial permeability transition. EMBO Rep. 2017;18:1065–76.
26. Rhee S, Kil I. Multiple Functions and Regulation of Mammalian Peroxiredoxins. Annual review of biochemistry. 2017;86:749–75.
27. Tu D, Jiang M, Gu W, Zhou Y, Zhu Q, Zhou Z, Chen Y, Shu M. Identification and characterization of atypical 2-cysteine peroxiredoxins from mud crab Scylla paramamosain: The first evidence of two peroxiredoxin 5 genes in non-primate species and their involvement in immune defense against pathogen infection. Fish Shellfish Immunol. 2017;69:119–27.
28. Arcaro A, Daga M, Cetrangolo G, Ciamporcero E, Lepore A, Pizzimenti S, Petrella C, Graf M, Uchida K, Mamone G, et al. Generation of Adducts of 4-Hydroxy-2-nonenal with Heat Shock 60 kDa Protein 1 in Human Promyelocytic HL-60 and Monocytic THP-1 Cell Lines. Oxidative medicine and cellular longevity. 2015: 296146.

Tables

TABLE 1 | Summary of downregulated proteins in A549 cells infected with influenza A H5N1 virus compared to H9N2-infected cells at 24 hpi ($r > 2$, $p < 0.05$).

Spot No.	Accession No.	gene	Protein name	MW (Da)	pI	Score
1	P04264	KRT1	Keratin, type II cytoskeletal 1	66170	8.15	120
2	P10809	HSPD1	60-kDa heat shock protein, mitochondrial	61187	5.7	69
3	B4DEF7	N /A	cDNA FLJ60062, highly similar to 78-kDa glucose-regulated protein	30458	5.77	68
4	Q59FC6	N /A	Tumor rejection antigen (Gp96) 1 variant	66140	5.08	46
5	V9HWE1	HEL113	Epididymis luminal protein 113	53676	5.24	156
6	Q7L4M3	KRT 8	KRT8 protein	30802	5.05	57
7	P07237	P4HB	Protein disulfide-isomerase	57146	5.96	60
8	P06576	ATP5F1B	ATP synthase subunit beta, mitochondrial	56525	5.26	130
9	Q9UJZ1	STOML2	Stomatin-like protein 2, mitochondrial	38839	4.45	120
10	P35908	KRT2	Keratin, type II cytoskeletal 2 epidermal	65678	8.07	47
11	P13645	KRT10	Keratin, type I cytoskeletal 10	58994	5.13	49
12	A8K401	PHB	Prohibitin, isoform CRA_a	29843	4.14	175
13	P30044	PRDX5	Peroxiredoxin-5, mitochondrial	17611	9.02	50
14	Q9BYX7	POTEKP	Putative beta-actin-like protein 3	42331	5.91	53
15	Q6FHZ0	MDH2	Malate dehydrogenase, mitochondrial	35965	8.92	63
16	P38646	HSPA9	Stress-70 protein, mitochondrial	73967	6.03	52

TABLE 2 | Summary of upregulated proteins in A549 cells infected with influenza A H5N1 virus compared to H9N2-infected cells at 24 hpi ($r > 2$, $p < 0.05$).

Spot No.	Accession No.	gene	Protein name	MW (Da)	pI	Score
17	P30084	ECHS1	Enoyl-CoA hydratase, mitochondrial	31716	6.05	68
18	P02768	ALB	Serum albumin	47098	5.92	64
19	P35527	KRT9	Keratin, type I cytoskeletal 9	62255	5.14	72
20	Q9HC85	MB2	Metastasis related protein	10414	5.16	35
21	P11021	HSPA5	Endoplasmic reticulum chaperone BiP	71002	5.23	155
22	AIZ70879	N/A	immunoglobulin heavy chain variable region, partial	8328	11.84	42
23	P34931	HSPA1L	heat shock 70-kDa protein 1-like	77913	7.55	64
24	A0A1L1UHR1	HTL-T-186e	Homo sapiens sperm binding protein 1aing mRNA	30868	8.62	46
25	P09651	HNRNPA1	Heterogeneous nuclear ribonucleoprotein A1	34289	9.27	58
26	P22626	HNRNPA2B1	Heterogeneous nuclear ribonucleoproteins A2/B1	36041	8.67	52
27	P08670	VIM	vimentin isoform 1, partial	53676	5.06	56
28	Q8N1N4	KRT78	Keratin, type II cytoskeletal 78	57728	5.79	51
29	Q86Y46	KRT73	Keratin, type II cytoskeletal 73	42270	8.42	51
30	D9YZU9	HBG2	TPA: globin B2	16173	6.64	50
31	P68871	HBB	Beta globin	11534	5.9	46
32	P69905	HBA1	Hemoglobin subunit alpha	15174	8.73	65

Figures

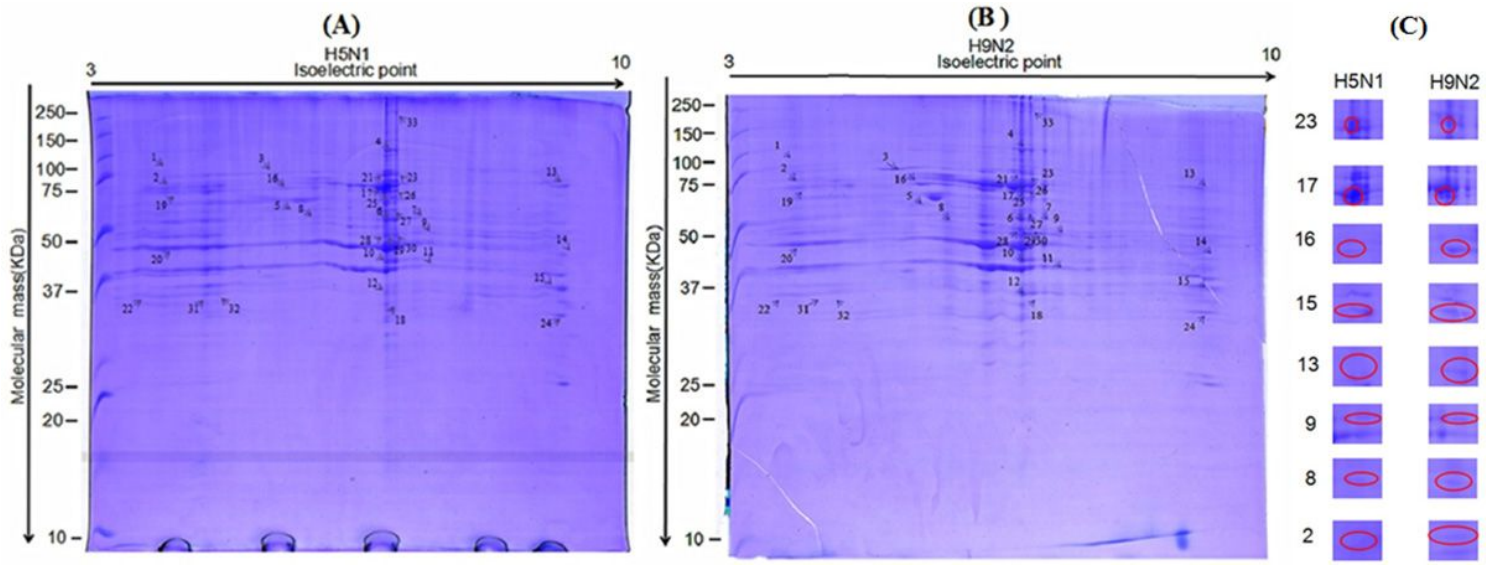

Figure 1

2-DE gel images of H9N2-infected and H5N1 groups of A549 cells at 24 hpi. a 2-DE gel of the H9N2-infected group. b 2-DE gel of the H5N1-infected group. The distribution of differential protein spots

identified by mass spectrometry in the two-dimensional electrophoresis pattern. The downward arrow indicates that H5N1 expressed down-regulated protein spots compared to the low-toxic control; the upward arrow indicates that H5N1 expressed up-regulated protein spots compared to the low-toxic control. c Enlarged regions of several differentially expressed protein spots. Differentially expressed protein spots are indicated by numbers and circles.

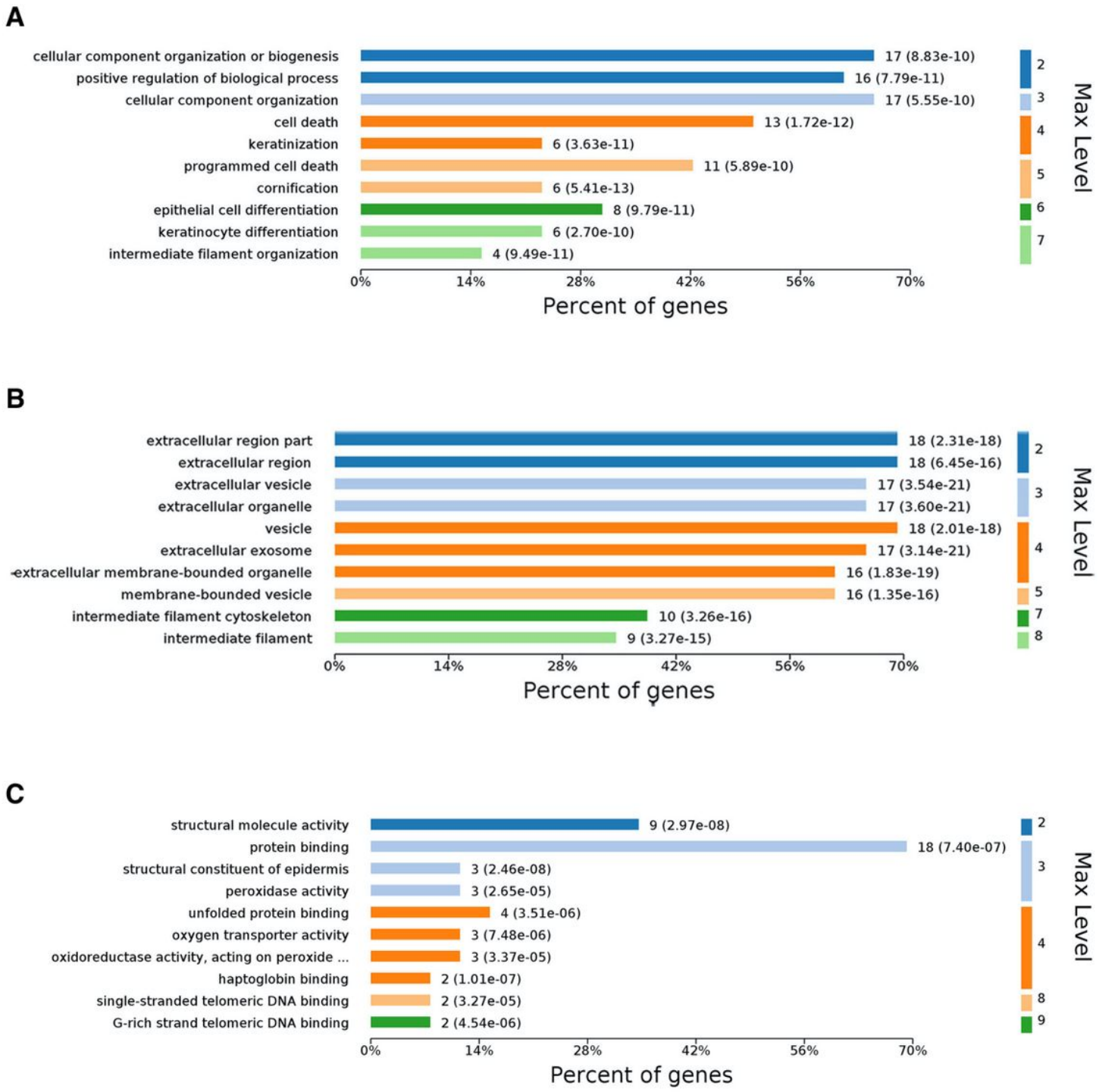

Figure 2

Differentially expressed protein GO annotation. a Biological Process. b Cell Component. c Molecular Function.

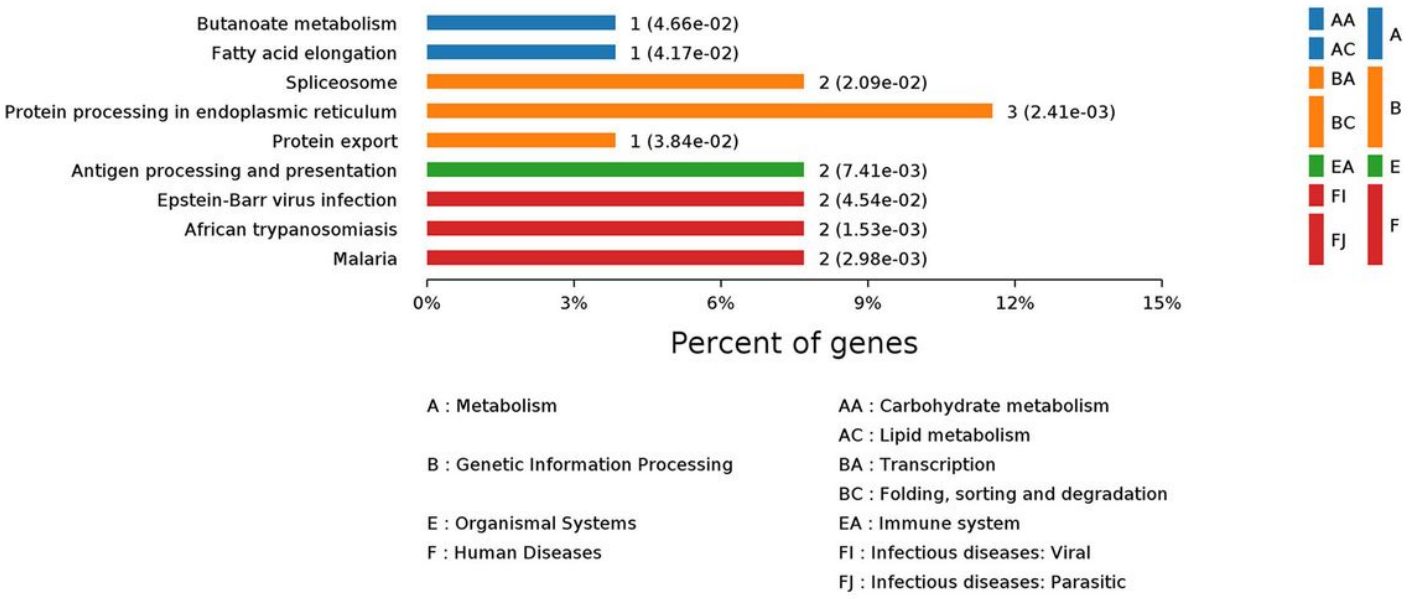

Figure 3

Analysis of differentially expressed proteins in KEGG signaling pathways.

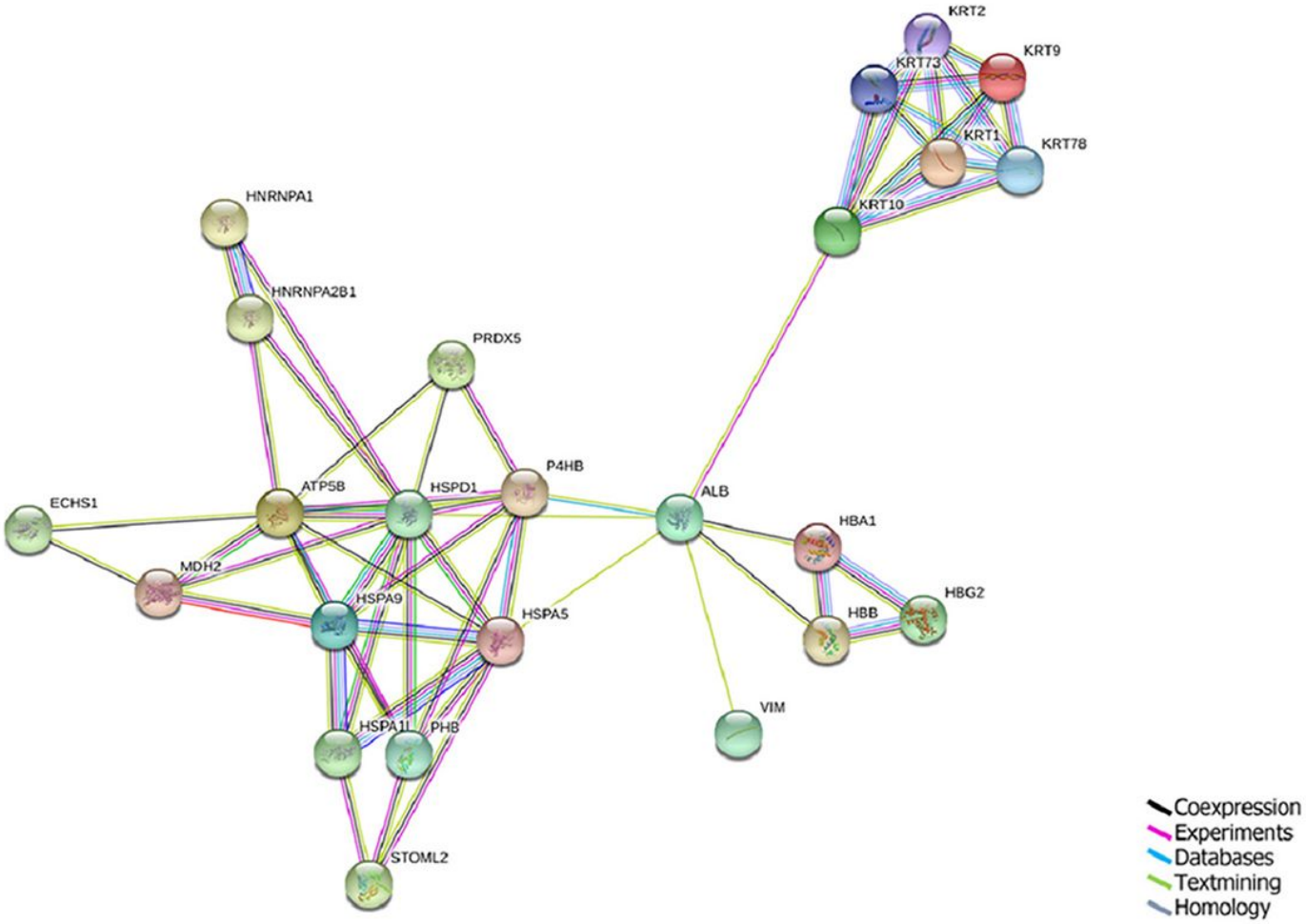

Figure 4

Protein interaction network diagrams at 24 h were analyzed by String software. Colored lines denote interactions.

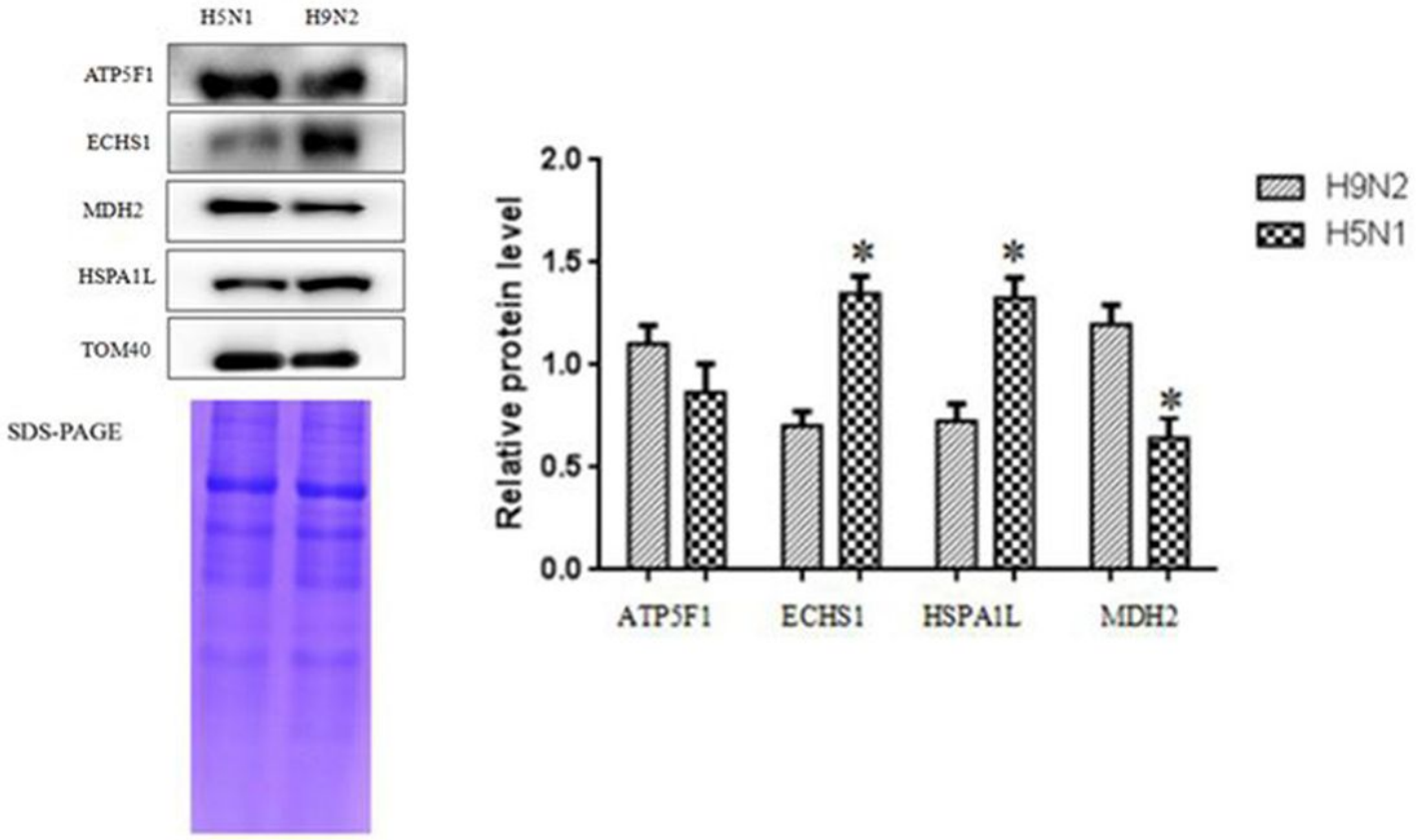

Figure 5

Effects of H9N2 and H5N1 infections on ATP5F1, ECHS1, HSPA1L and MDH2 mitochondria protein expression in A549 cells.*, $p<0.05$ vs. H9N2-infected group; n=3.

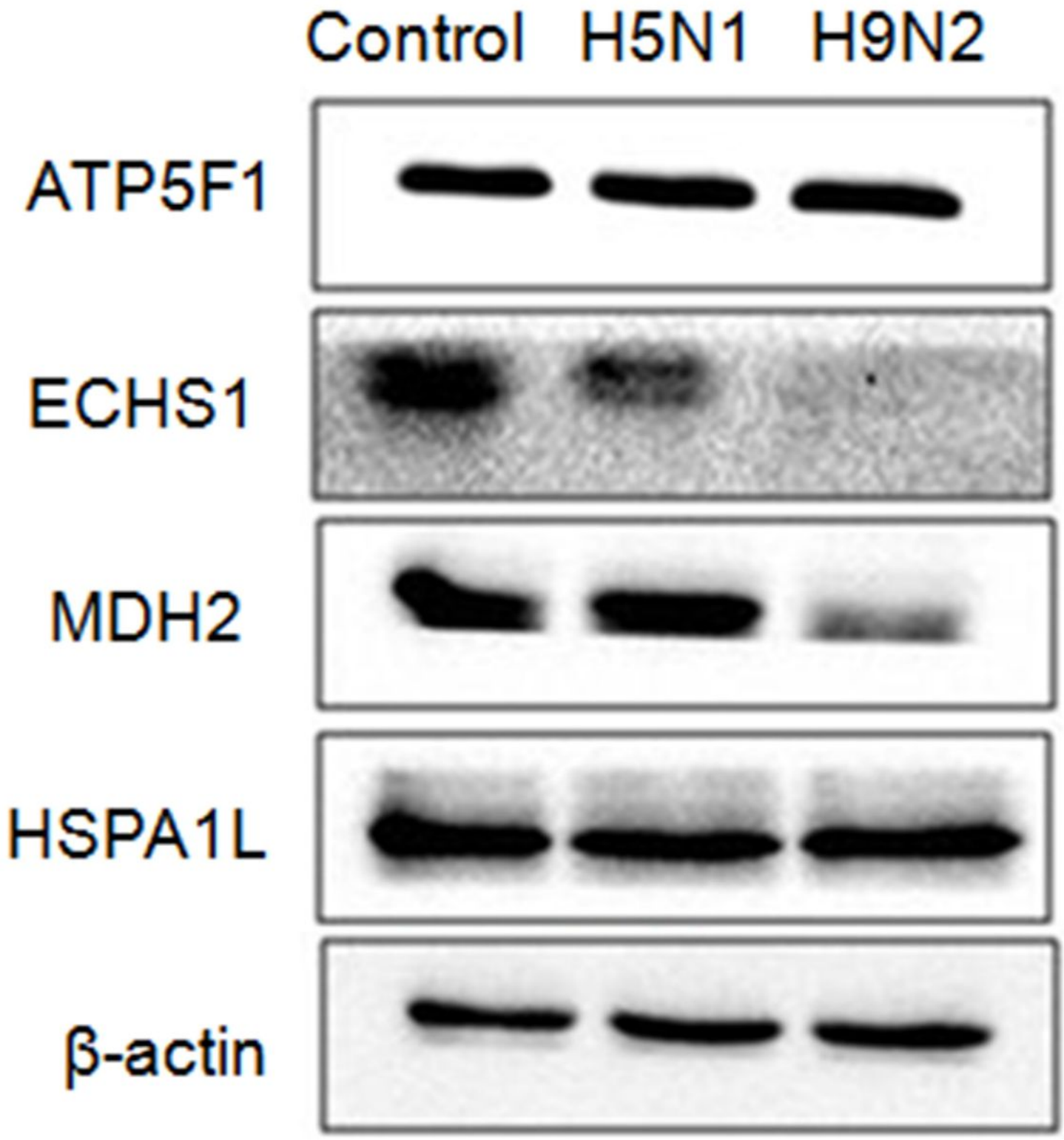

Figure 6

Effects of H9N2 and H5N1 infections on ATP5F1, ECHS1, HSPA1L and MDH2 total protein expression in A549 cells.

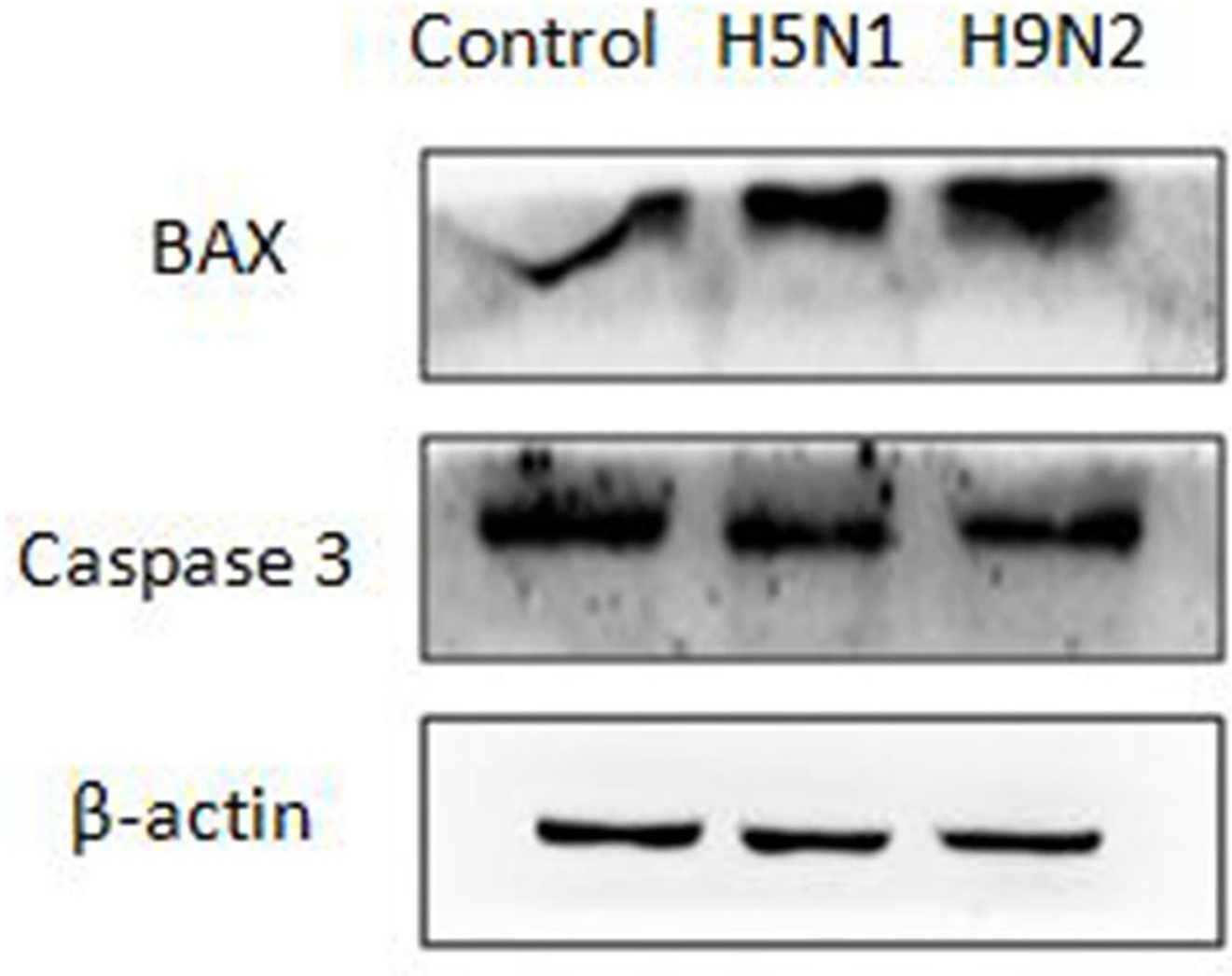

Figure 7

Western blot analysis of BAX and Caspase 3 protein levels in normal A549 cells and H5N1- and H9N2-infected A549 cells. β-actin was used as an internal reference.

Supplementary Files

This is a list of supplementary files associated with this preprint. Click to download.

- TableSupplementarymaterial.doc